AIAA XXX

Attitude Parameter Inspired Descriptions of Relative Orbital Motion

Erik A. Hogan and Hanspeter Schaub

University of Colorado at Boulder, Boulder, CO, 80309, USA

AIAA/AAS Astrodynamics Specialist Conference, Minneapolis, MN, August 13–16, 2012

Attitude Parameter Inspired Descriptions of Relative Orbital Motion

Erik A. Hogan* and Hanspeter Schaub†
University of Colorado at Boulder, Boulder, CO, 80309, USA

This paper describes the development of novel relative orbital motion descriptions for a two craft formation, defined by a separation distance and relative orientation parameter set. These descriptions allow for the use of separation distance as a state parameter for the relative motion, while avoiding singularity issues that plague spherical coordinate descriptions. Instead, Euler parameter- or modified Rodrigues parameter-like coordinates are employed to describe the relative orientation. Equations of motion are developed that allow propagation of these new descriptions for the case of a circular reference orbit and small separation distances between the craft. Feedback control laws are developed to stabilize the relative motion between the craft. Numerical simulation is used to compare the newly developed relative motion descriptions with inertial equations of motion. The results validate these new descriptions as a practical method for describing relative motion.

I Introduction

In relative motion studies of spacecraft formations, the Hill frame coordinates are a commonly used relative position and velocity description between a chief and a deputy craft. These coordinates are a cartesian description, and applying them to the special case of a circular chief orbit with small separation distances results in the Clohessy-Wiltshire (CW) equations.[1] For some applications, a curvilinear coordinate frame is preferred and used to describe the relative motion; this curvilinear coordinate frame is typically a spherical frame, defined by the separation distance between the craft and two angles which provide information about the orientation of the line of sight vector from the chief to deputy.[2] Another relative motion description uses differential orbital elements.[3,4] Here, one craft in the formation is specified as the reference craft, and all other craft in the formation are defined by differencing their orbital elements with those of the reference.

In the current study, motion with respect to a circular chief orbit will be investigated using an alternative relative position description. In some cases, relative motion descriptions are sought which use the separation distance between chief and deputy as a coordinate. This can be important for certain applications where the separation distance has a direct impact on the dynamics and control of the formation, or where collision is a real possibility. One such application where these concerns are applicable is found in References 5. Here, electrostatic forces are used to generate a contactless tugging force between chief and deputy, allowing the chief to thrust and tow the deputy into a new orbit.[6,7] Further, the ion-sheppard method of large debris removal method also requires close proximity flying on the order of dozens of meter where the separation distance errors should be controlled more strongly than the relative heading errors.[8–10] To develop the relative motion control law, spherical coordinates are chosen because the separation distance appears directly in the electrostatic force expression. Thus, it is advantageous for the distance between deputy and chief to appear as a state in the relative equations of motion. Furthermore, spherical coordinates provide a simple way to prescribe relative trajectories in which the chief maneuvers around the deputy while maintaing a safe separation distance, as only the angles need modification during the maneuver. Using a spherical coordinate system to describe the relative motion results in kinematic singularities, however; it is of interest to study other potential relative position descriptions which may avoid these issues. By deriving the relative motion using alternate descriptions, new dynamical equations are obtained which have potentially advantageous properties.

*Graduate Student, University of Colorado at Boulder
†Associate Professor, H. Joseph Smead Fellow, Aerospace Engineering Sciences, University of Colorado, Chief Technologist, Wacari Group, Boulder, CO

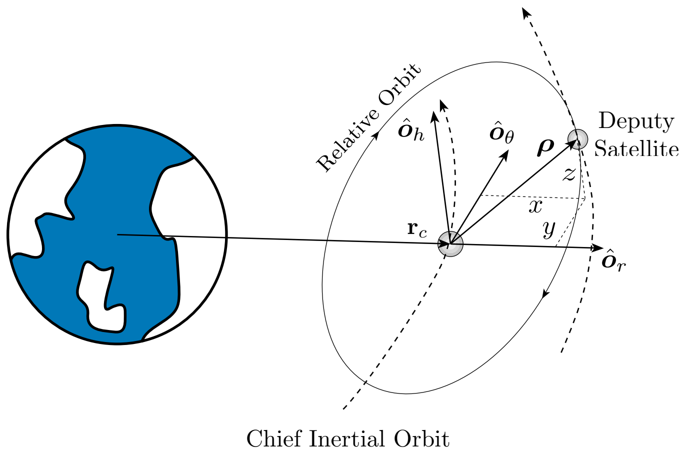

Figure 1: Relative motion of deputy and chief, illustrated using rotating Hill frame

When using spherical coordinates, kinematic singularities may appear depending on how the angles are defined. For example, in Reference 2 no singularities are encountered because the spherical frame is defined relative to an inertial frame, and the equations are linearized. In Reference 5, however, the spherical frame is defined relative to the rotating Hill frame and kinematic singularities result because arbitrary relative motion is considered. In spite of these singularities, the spherical frame is used because it contains the separation distance as a state. In the current study, alternate relative motion descriptions are sought which use separation distance as state but avoid the singularities associated with using spherical coordinates. To that end, one relative position description, inspired by the Euler parameter attitude set, is proposed which uses a once-redundant set of parameters to describe the relative orientation of the craft in the formation. The relative orientation is parameterized using the components of the unit-vector which points from chief to deputy. Beyond this unit-vector description, a relative motion description is constructed which contains two possible sets of parameters for describing the relative orientation in conjunction with the separation distance. While these two possible sets contain singularities, these singularities do not occur at the same relative orientation, very similar to the behavior of the modified Rodrigues parameter attitude description.[11–14] Thus, a switching condition may be employed to avoid these singularities all together. Beyond developing and analyzing the corresponding equations of motion for these new relative motion descriptions, control laws employing continuous feedback are derived to stabilize the relative motion.

The paper is structured as follows. First, background information regarding relative orbital motion is provided, including the Clohessy-Wiltshire equations. Then, the unit-vector description is introduced and its equations of motion are derived. Next, the $\boldsymbol{\sigma}$ set is defined and its corresponding dynamical equations are obtained. Control laws for reference trajectory tracking are developed, and numerical simulation is used to illustrate their performance.

II Background

In this paper, the relative motion of a deputy satellite with respect to a chief is studied. This scenario is depicted in Figure 1. Here, $\boldsymbol{r}_c$ describes the inertial position of the chief and $\boldsymbol{r}_d$ describes the position of the deputy. The relative position, $\boldsymbol{\rho}$, is defined as

$$\boldsymbol{\rho} = \boldsymbol{r}_d - \boldsymbol{r}_c. \tag{1}$$

Of interest is how this relative position evolves under the influence of natural orbital motion and a deputy control input. One relative motion description frequently used is the cartesian Hill-frame coordinate system, illustrated in Figure 1. The axes of the Hill frame, denoted as $\mathcal{H}$, are computed using

$$\hat{\boldsymbol{o}}_r = \frac{\boldsymbol{r}}{r},\ \hat{\boldsymbol{o}}_\theta = \hat{\boldsymbol{o}}_h \times \hat{\boldsymbol{o}}_r,\ \hat{\boldsymbol{o}}_h = \frac{\boldsymbol{r} \times \dot{\boldsymbol{r}}}{|\boldsymbol{r} \times \dot{\boldsymbol{r}}|}. \tag{2}$$

The Hill frame is convenient for describing relative motion because the inertial position of the chief object is described completely by

$$\boldsymbol{r}_c = r_c \hat{\boldsymbol{o}}_r. \tag{3}$$

Furthermore, the angular velocity of the Hill frame with respect to an inertial frame is given by

$$\boldsymbol{\omega}_{\mathcal{H}/\mathcal{N}} = \dot{f} \hat{\boldsymbol{o}}_h, \tag{4}$$

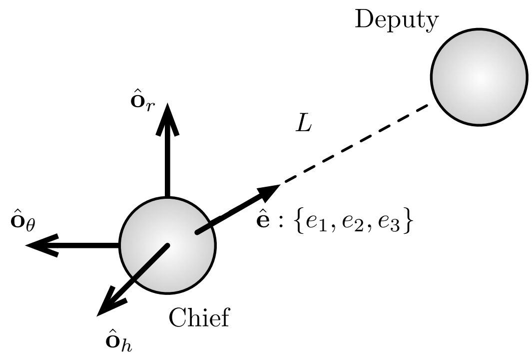

Figure 2: Unit-vector description of relative motion

where the script $\mathcal{N}$ refers to an inertial frame, and $\dot{f}$ is the instantaneous true anomaly rate. Using the Hill frame, the position of the deputy craft may be expressed as

$$\boldsymbol{r}_d = \boldsymbol{r}_c + \boldsymbol{\rho} = (r_c + x)\hat{\boldsymbol{o}}_r + y\hat{\boldsymbol{o}}_\theta + z\hat{\boldsymbol{o}}_h, \tag{5}$$

where x,y, and z are Hill frame components of the relative position vector $\boldsymbol{\rho}$. Using this Hill-frame description, the relative equations of motion are found to be[15]

$$\ddot{x} - 2\dot{f}\left(\dot{y} - y\frac{\dot{r}_c}{r_c}\right) - x\dot{f}^2 - \frac{\mu}{r_c^2} = -\frac{\mu}{r_d^3}(r_c + x) \tag{6a}$$

$$\ddot{y} + 2\dot{f}\left(\dot{x} - x\frac{\dot{r}_c}{r_c}\right) - y\dot{f}^2 = -\frac{\mu}{r_d^3}y \tag{6b}$$

$$\ddot{z} = -\frac{\mu}{r_d^3}z \tag{6c}$$

In Eq. (6) no assumptions have been made about the distance between deputy and chief, and no restrictions have been placed on the chief orbit. Thus, these equations are valid for arbitrary relative motion. In many formation flying applications, it is of interest to consider flying the deputy and chief at separation distances much smaller than their inertial orbit radii. This allows for a linearization of Eq. 6 about the chief motion. If only the case of circular chief motion is considered, the true anomaly rate is constant and determined by

$$\dot{f} = \text{constant} = \sqrt{\frac{\mu}{r_c^3}} = n. \tag{7}$$

Under these assumptions, the relative equations of motion may be simplified to the well-known Clohessy-Wiltshire (CW) equations[1]

$$\ddot{x} - 2n\dot{y} - 3n^2x = 0 \tag{8a}$$

$$\ddot{y} + 2n\dot{x} = 0 \tag{8b}$$

$$\ddot{z} + n^2z = 0. \tag{8c}$$

The CW equations are useful because they have an analytic solution as a function of initial conditions. There are drawbacks, however, that one may encounter when working with these equations. Because the Hill-frame description is cartesian in nature, and orbits form a curvilinear space, the CW equations will not accurately capture the relative motion for moderately large separation distances. This is due to the fact that the local curvature of the orbit is approximated as linear.

III Relative Orbit Descriptions using Heading and Separation Measures

III.A The Unit-vector Description

Depending on the particular application, alternate relative motion descriptions may be desired. It is sometimes of interest to use the separation distance between the craft directly as a coordinate, breaking up the description of relative

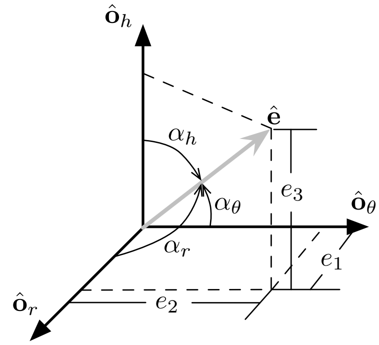

Figure 3: The unit-vector components are equivalent to the cosines of the angles between $\hat{e}$ and the Hill frame axes

motion into a distance and relative orientation measure. To avoid the singularity issues associated with a spherical coordinate description, an alternate method is proposed which uses the separation distance, $L = \rho$, and the unit-vector pointing from chief to deputy, as illustrated in Figure 2. This unit-vector is defined as

$$\hat{\boldsymbol{e}} = \frac{\boldsymbol{\rho}}{\rho}. \tag{9}$$

Using this description, the position of the deputy with respect to the chief in Hill frame components is given by

$$\boldsymbol{\rho} = Le_1\hat{\boldsymbol{o}}_r + Le_2\hat{\boldsymbol{o}}_\theta + Le_3\hat{\boldsymbol{o}}_h, \tag{10}$$

where e_i are the Hill frame components of $\hat{\boldsymbol{e}}$. The forward and inverse mapping between the cartesian Hill frame components and the unit-vector description is given by

$$\begin{bmatrix} x \\ y \\ z \end{bmatrix} = \begin{bmatrix} Le_1 \\ Le_2 \\ Le_3 \end{bmatrix}, \quad \begin{bmatrix} e_1 \\ e_2 \\ e_3 \end{bmatrix} = \begin{bmatrix} x/L \\ y/L \\ z/L \end{bmatrix} \tag{11}$$

with

$$L^2 = x^2 + y^2 + z^2. \tag{12}$$

The conversion between the rates is given by

$$\begin{bmatrix} \dot{x} \\ \dot{y} \\ \dot{z} \end{bmatrix} = \begin{bmatrix} \dot{L}e_1 + L\dot{e}_1 \\ \dot{L}e_2 + L\dot{e}_2 \\ \dot{L}e_3 + L\dot{e}_3 \end{bmatrix}, \quad \begin{bmatrix} \dot{e}_1 \\ \dot{e}_2 \\ \dot{e}_3 \end{bmatrix} = \begin{bmatrix} (\dot{x} - \dot{L}e_1)/L \\ (\dot{y} - \dot{L}e_2)/L \\ (\dot{z} - \dot{L}e_3)/L \end{bmatrix} \tag{13}$$

with the separation-distance rate determined as

$$\dot{L} = \frac{x\dot{x} + y\dot{y} + z\dot{z}}{L}. \tag{14}$$

Geometrically, the components e_i may be interpreted as angle measures between the unit-vector $\hat{\boldsymbol{e}}$ and the Hill-frame axes $\hat{\boldsymbol{o}}_r$, $\hat{\boldsymbol{o}}_\theta$, and $\hat{\boldsymbol{o}}_h$. More specifically, they represent the direction cosines of $\hat{\boldsymbol{e}}$ with respect to the Hill frame. If the angle between $\hat{\boldsymbol{e}}$ and the $\hat{\boldsymbol{o}}_i$ axis is denoted as α_i, as illustrated in Figure 3, then the components of $\hat{\boldsymbol{e}}$ are equivalent to

$$\begin{bmatrix} e_1 \\ e_2 \\ e_3 \end{bmatrix} = \begin{bmatrix} \cos\alpha_r \\ \cos\alpha_\theta \\ \cos\alpha_h \end{bmatrix}. \tag{15}$$

Considering the relationship between the cartesian Hill frame coordinates and the unit-vector description, an apparent singularity occurs at $L = 0$. This singularity is a result of the non-uniqueness of the unit-vector at this separation distance. In fact, when the separation distance is zero, any arbitrary unit-vector will appropriately convert the unit-vector description into the cartesian coordinates. While this presents an issue mathematically, it is of little practical concern because a separation distance of zero is impossible with actual craft. The unit-vector description is well defined everywhere else, and is thus a good candidate for describing arbitrary relative motion.

With the unit-vector description, four parameters are used to describe a three-dimensional location. Similar to the use of the 4-dimensional Euler parameter (EP) set to describe a three dimensional attitude, there must be a constraint on the parameters. In this case, the unity constraint

$$e_1^2 + e_2^2 + e_3^2 = 1 \tag{16}$$

must be satisfied at all times. Differentiating this constraint twice with respect to time yields

$$e_1\ddot{e}_1 + e_2\ddot{e}_2 + e_3\ddot{e}_3 + \dot{e}_1^2 + \dot{e}_2^2 + \dot{e}_3^2 = 0. \tag{17}$$

Considering Eq. (17), it appears that singularities may present a problem when one of the vector components is zero. However, when combined with the relative motion differential equations, this singularity will vanish.

Another parallel with the Euler parameter attitude description is the issue of uniqueness. When the four dimensional Euler parameters are used to describe attitude, there are two sets that describe the same orientation. With the unit-vector relative motion description, there are two sets of parameters that describe the exact same relative position. In addition to the $\boldsymbol{\rho} = L\hat{e}$ description detailed above, the same location may be obtained using $\boldsymbol{\rho} = -L(-\hat{\boldsymbol{e}})$. This non-uniqueness has an important implication for the $\boldsymbol{\sigma}$ set introduced later in the paper.

To determine the relative equations of motion, Eqs. (11) and (13) are substituted into Eq. (8) and the constraint in Eq (17) is used to yield

$$\begin{bmatrix} \ddot{L} \\ \ddot{e}_1 \\ \ddot{e}_2 \\ \ddot{e}_3 \end{bmatrix} = [f(L, \dot{L}, \hat{\boldsymbol{e}}, \dot{\hat{\boldsymbol{e}}})] + [G_e]\boldsymbol{u} \tag{18}$$

where

$$[f(L, \dot{L}, \hat{\boldsymbol{e}}, \dot{\hat{\boldsymbol{e}}})] = \begin{bmatrix} L\left(2n(e_1\dot{e}_2 - e_2\dot{e}_1) + n^2(3{e_1}^2 - {e_3}^2) + \dot{e}_1^2 + \dot{e}_2^2 + \dot{e}_3^2\right) \\ e_1\left(2ne_2\dot{e}_1 + n^2\left(3{e_2}^2 + 4{e_3}^2\right) - \dot{e}_1^2 - \dot{e}_2^2 - \dot{e}_3^2\right) - 2n{e_1}^2\dot{e}_2 + 2n\dot{e}_2 + 2\frac{\dot{L}}{L}\left(ne_2 - \dot{e}_1\right) \\ e_2\left(2n(e_2\dot{e}_1 - e_1\dot{e}_2) + n^2({e_3}^2 - 3{e_1}^2) - \dot{e}_1^2 - \dot{e}_2^2 - \dot{e}_3^2\right) - 2n\dot{e}_1 - 2\frac{\dot{L}}{L}\left(ne_1 + \dot{e}_2\right) \\ -e_3\left(\left(\dot{e}_1 - ne_2\right)^2 + 2ne_1\dot{e}_2 + 4n^2{e_1}^2 + \dot{e}_2^2 + \dot{e}_3^2\right) - 2\dot{e}_3\frac{\dot{L}}{L} \end{bmatrix} \tag{19a}$$

$$[G_e] = \frac{1}{L}\begin{bmatrix} Le_1 & Le_2 & Le_3 \\ 1 - e_1^2 & -e_1e_2 & -e_1e_3 \\ -e_1e_2 & 1 - e_2^2 & -e_2e_3 \\ -e_1e_3 & -e_2e_3 & 1 - e_3^2 \end{bmatrix} = \begin{bmatrix} \hat{\boldsymbol{e}}^T \\ \frac{1}{L}\left([I] - \hat{\boldsymbol{e}}\hat{\boldsymbol{e}}^T\right) \end{bmatrix} \tag{19b}$$

$$\boldsymbol{u} = \begin{bmatrix} u_x \\ u_y \\ u_z \end{bmatrix} \tag{19c}$$

Note that the only singularity in Eq. (18) occurs when $L = 0$. For reasons discussed above, this is of little concern for the scope of this study. The unit-vector description provides practically non-singular equations of motion that use the separation distance and a redundant set of orientation parameters to describe relative motion. In this manner, the singular issues that plague the spherical frame description are avoided while still maintaining a direct measure of the distance between the deputy and chief.

III.B The σ-Set Relative Motion Description

The unit-vector description detailed previously is inspired by the Euler parameter attitude description. Now, an additional relative motion description is considered which is inspired by modified Rodrigues parameters (MRPs).[15] The unit-vector description is used to define new orientation parameters that reduce the relative motion description from 4 parameters ($\boldsymbol{L}$, $\hat{\boldsymbol{e}}$) to three. Similar to the manner in which MRPs are defined using the Euler parameter set, a new relative motion orientation description is defined using the unit-vector components. The $\boldsymbol{\sigma}$ set contains L, the separation distance, and two orientation parameters defined as

$$\begin{bmatrix} \sigma_1 \\ \sigma_2 \end{bmatrix} = \frac{1}{1 + e_1}\begin{bmatrix} e_2 \\ e_3 \end{bmatrix} \tag{20}$$

The once-redundant unit-vector description is used to define a new, minimal-set description of relative motion. The inverse mapping from the $\boldsymbol{\sigma}$-set to unit-vector components is

$$\begin{bmatrix} e_1 \\ e_2 \\ e_3 \end{bmatrix} = \frac{1}{1+\sigma^2} \begin{bmatrix} 1-\sigma^2 \\ 2\sigma_1 \\ 2\sigma_2 \end{bmatrix}, \tag{21}$$

where $\sigma^2 = \sigma_1^2 + \sigma_2^2$. Using Eq. (11), the mapping between $\boldsymbol{\sigma}$-set and Hill frame coordinates is determined to be

$$\begin{bmatrix} x \\ y \\ z \end{bmatrix} = \frac{L}{1+\sigma^2} \begin{bmatrix} 1-\sigma^2 \\ 2\sigma_1 \\ 2\sigma_2 \end{bmatrix}. \tag{22}$$

Taking the derivative with respect to time yields the velocity mapping

$$\begin{bmatrix} \dot{x} \\ \dot{y} \\ \dot{z} \end{bmatrix} = \frac{\dot{L}}{1+\sigma^2} \begin{bmatrix} 1-\sigma^2 \\ 2\sigma_1 \\ 2\sigma_2 \end{bmatrix} + \frac{2L}{(1+\sigma^2)^2} \begin{bmatrix} -2\dot{\boldsymbol{\sigma}}^T\boldsymbol{\sigma} \\ (1-\sigma_1^2+\sigma_2^2)\dot{\sigma}_1 - 2\sigma_1\sigma_2\dot{\sigma}_2 \\ (1+\sigma_1^2-\sigma_2^2)\dot{\sigma}_2 - 2\sigma_1\sigma_2\dot{\sigma}_1 \end{bmatrix}. \tag{23}$$

Inverting the above relationships, the mapping from Hill-frame coordinates to $\boldsymbol{\sigma}$-set is found to be

$$\begin{bmatrix} \sigma_1 \\ \sigma_2 \end{bmatrix} = \frac{1}{x+L} \begin{bmatrix} y \\ z \end{bmatrix}, \tag{24}$$

with the corresponding velocity mapping

$$\begin{bmatrix} \dot{\sigma}_1 \\ \dot{\sigma}_2 \end{bmatrix} = \frac{1}{x+L} \begin{bmatrix} \dot{y} \\ \dot{z} \end{bmatrix} - \frac{\dot{x}+\dot{L}}{(x+L)^2} \begin{bmatrix} y \\ z \end{bmatrix}. \tag{25}$$

To obtain the equations of motion for the $\boldsymbol{\sigma}$ set, the above relationships are inserted into the CW equations. The result is expressed in the form

$$\begin{bmatrix} \ddot{L} \\ \ddot{\boldsymbol{\sigma}} \end{bmatrix} = [h(L, \dot{L}, \boldsymbol{\sigma}, \dot{\boldsymbol{\sigma}})] + [G_\sigma]\boldsymbol{u}. \tag{26}$$

The three components of the $[h]$ matrix are

$$\begin{aligned} h_L = \frac{L}{(1+\sigma^2)^2} \Big[& 3n^2(\sigma_1^4 + \sigma_2^4 + 1) + 4\dot{\sigma}_1 n - 2n\sigma_2^2(5n + 2\dot{\sigma}_1) + 2n\sigma_1^2(3n(-1+\sigma_2^2) + 2\dot{\sigma}_1) \\ & + 8n\sigma_1\sigma_2\dot{\sigma}_2 + 4\dot{\boldsymbol{\sigma}}^T\dot{\boldsymbol{\sigma}} \Big] \end{aligned} \tag{27a}$$

$$\begin{aligned} h_{\sigma_1} = -\frac{1}{2L(1+\sigma^2)} \Big[& -6n^2L\sigma_1^3 + 2n\sigma_1^4\dot{L} + 4\sigma_1^2\dot{L}(n+\dot{\sigma}_1) - \left(1+\sigma_2^2\right)\dot{L}\left(2n\sigma_2^2 - 2(n+2\dot{\sigma}_1)\right) \\ & - 8L\sigma_2(n+\dot{\sigma}_1)\dot{\sigma}_2 + 2L\sigma_1\left(3n^2 - 5n^2\sigma_2^2 - 2\dot{\sigma}_1^2 + 2\dot{\sigma}_2^2\right) \Big] \end{aligned} \tag{27b}$$

$$\begin{aligned} h_{\sigma_2} = \frac{1}{2L(1+\sigma^2)} \Big[& -4n\sigma_1^3\sigma_2\dot{L} - 4n\sigma_1\left(\sigma_2+\sigma_2^3\right)\dot{L} - 4\dot{L}\dot{\sigma}_2 + 8L\sigma_1\dot{\sigma}_1\dot{\sigma}_2 + 2\sigma_1^2\left(2n^2L\sigma_2 - 2\dot{L}\dot{\sigma}_2\right) \\ & - \sigma_2\left(4\sigma_2\dot{L}\dot{\sigma}_2 + 4L\left(2n^2\left(1-\sigma_2^2\right) + 2n\dot{\sigma}_1 + \dot{\sigma}_1^2 - \dot{\sigma}_2^2\right)\right) \Big], \end{aligned} \tag{27c}$$

and the control sensitivity matrix is

$$[G_\sigma] = \begin{bmatrix} \frac{1-\sigma^2}{1+\sigma^2} & \frac{2\sigma_1}{1+\sigma^2} & \frac{2\sigma_2}{1+\sigma^2} \\ -\frac{\sigma_1}{L} & \frac{1-\sigma_1^2+\sigma_2^2}{2L} & -\frac{\sigma_1\sigma_2}{L} \\ -\frac{\sigma_2}{L} & -\frac{\sigma_1\sigma_2}{L} & \frac{1+\sigma_1^2-\sigma_2^2}{2L} \end{bmatrix}. \tag{28}$$

The control vector $\boldsymbol{u}$ is defined the same as before, with components in the Hill frame. An examination of the $\boldsymbol{\sigma}$ set equations reveals singularities in two different positions. One occurs when $L = 0$, which corresponds to a collision between chief and deputy. As discussed previously, this is of little practical importance. The second singularity occurs when $x = -L$ (or $e_1 = -1$). This singularity must be given attention, as there are many possible trajectories which may encounter this configuration.

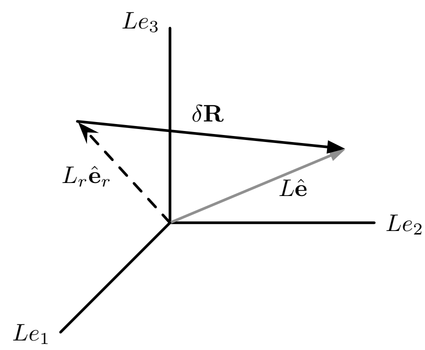

Figure 4: The tracking error measure δR is the vector from the reference location to the current deputy position

III.C The σ Shadow Set

As with the unit-vector description, there are two sets of L and $\boldsymbol{\sigma}$ values that describe the same relative position. This phenomenon is similar to the existence of a shadow set in the Modified Rodrigues parameter attitude description.[15] Using the alternate unit-vector description ($-L$,-$\hat{\boldsymbol{e}}$), the alternate $\boldsymbol{\sigma}$ set may be found. This shadow set, denoted as $\boldsymbol{\sigma}_s$, is defined as

$$\boldsymbol{\sigma}_s = -\frac{\boldsymbol{\sigma}}{\sigma^2}. \tag{29}$$

Differentiating yields the shadow set velocity

$$\dot{\boldsymbol{\sigma}}_s = -\frac{\dot{\boldsymbol{\sigma}}}{\sigma^2} + 2\frac{\boldsymbol{\sigma}^T\dot{\boldsymbol{\sigma}}}{\sigma^4}\boldsymbol{\sigma}, \tag{30}$$

where $\sigma^4 = (\sigma_1^2 + \sigma_2^2)^2$. For any relative motion, a set of $-L$, $-\dot{L}$, $\boldsymbol{\sigma}_s$, and $\dot{\boldsymbol{\sigma}}_s$ describes the exact same relative position and velocity as L, $\dot{L}$, $\boldsymbol{\sigma}$ and $\dot{\boldsymbol{\sigma}}$. In fact, one may switch between the original and shadow set arbitrarily. Each set evolves according to the same differential equations.

This has important implications regarding the singularity at $x = -L$. If this singularity is approaching, a switch to the shadow set may be used to avoid it. When the original set is at the singularity, the shadow set is well defined at $\boldsymbol{\sigma} = \mathbf{0}$. By choosing an appropriate switching location, arbitrary relative motion may be described using the $\boldsymbol{\sigma}$ set without encountering any singularities. Here, a switching condition of $\sigma^2 = 1$ is used. That is, when the magnitude of $\boldsymbol{\sigma}$ becomes larger than 1 a switch to the shadow set is employed. Considering the relationship between the unit-vector description and $\boldsymbol{\sigma}$ set, it can be shown that switching at this location restricts e_1 to only positive values, i.e. $e_1 > 0$. Changing back and forth between original and shadow set is equivalent to switching between L, $\hat{\boldsymbol{e}}$ and $-L$, $-\hat{\boldsymbol{e}}$.

IV Relative Motion Control

In this section relative motion control is considered, using both the unit-vector description and $\boldsymbol{\sigma}$ set. The goal is tracking an arbitrary deputy trajectory. Because the CW equations are used to derive the equations of motion for these descriptions, only trajectories with a chief-deputy separation distance of less than 1 km are considered. It is assumed that the necessary control acceleration, $\boldsymbol{u}$, is achievable by inertial thrusters.

IV.A Unit-vector Control

The most apparent obstacle present when using the unit-vector description for control is the fact that there are only three control inputs for a four dimensional system. However, the unit-vector components are not independent. Thus, it is possible to formulate the control problem in such a way as to obtain desired tracking behavior using the three control inputs.

IV.A.1 Hill-Frame Like Control

For the first control law approach, consider the vector $\boldsymbol{R}$ defined as

$$\boldsymbol{R} = L\hat{\boldsymbol{e}}, \tag{31}$$

with the associated derivatives

$$\dot{\boldsymbol{R}} = \dot{L}\hat{\boldsymbol{e}} \tag{32a}$$

$$\ddot{\boldsymbol{R}} = \ddot{L}\hat{\boldsymbol{e}} + 2\dot{L}\dot{\hat{\boldsymbol{e}}} + L\ddot{\hat{\boldsymbol{e}}} \tag{32b}$$

Note that the components of $\boldsymbol{R}$ are equivalent to the Cartesian Hill-frame components x, y, and z. Any set of L and $\hat{\boldsymbol{e}}$ will describe exactly one $\boldsymbol{R}$ vector. Thus, if the system tracks a desired L and $\hat{\boldsymbol{e}}$, then it will also track the equivalent $\boldsymbol{R}$. We may enforce tracking of L and $\hat{\boldsymbol{e}}$, then, by tracking the $\boldsymbol{R}_r$ vector, defined as

$$\boldsymbol{R}_r = L_r\hat{\boldsymbol{e}}_r, \tag{33}$$

where L_r and $\hat{\boldsymbol{e}}_r$ describe a desired reference trajectory. For the control law development, consider the candidate Lyapunov function[16]

$$V_1(\delta\boldsymbol{R}, \delta\dot{\boldsymbol{R}}) = \frac{1}{2}\delta\boldsymbol{R}^T[K]\delta\boldsymbol{R} + \frac{1}{2}\delta\dot{\boldsymbol{R}}^T\delta\dot{\boldsymbol{R}}, \tag{34}$$

where $\delta\boldsymbol{R} = \boldsymbol{R} - \boldsymbol{R}_r$ and $[K]$ is a positive definite gain matrix. Geometrically, the tracking error $\delta\boldsymbol{R}$ is the vector from the reference position to the actual position of the deputy, as illustrated in Figure 4. It makes sense, then, that driving this vector to $\boldsymbol{0}$ would lead to tracking of the reference trajectory. The derivative of the candidate Lyapunov function with respect to time is

$$\dot{V}_1(\delta\boldsymbol{R}, \delta\dot{\boldsymbol{R}}) = \delta\dot{\boldsymbol{R}}^T\left([K]\delta\boldsymbol{R} + \ddot{\boldsymbol{R}} - \ddot{\boldsymbol{R}}_r\right). \tag{35}$$

For the deputy motion, the acceleration of $\boldsymbol{R}$ is

$$\ddot{\boldsymbol{R}} = [f_R] + \boldsymbol{u} = \begin{bmatrix} 2n(\dot{L}e_2 + L\dot{e}_2) + 3n^2Le_1 \\ -2n(\dot{L}e_1 + L\dot{e}_1) \\ -n^2Le_3 \end{bmatrix} + \begin{bmatrix} u_x \\ u_y \\ u_z \end{bmatrix}. \tag{36}$$

Substituting this back into the Lyapunov rate function yields

$$\dot{V}_1(\delta\boldsymbol{R}, \delta\dot{\boldsymbol{R}}) = \delta\dot{\boldsymbol{R}}^T\left([K]\delta\boldsymbol{R} + [f_R] + \boldsymbol{u} - \ddot{\boldsymbol{R}}_r\right). \tag{37}$$

To ensure Lyapunov stability, the control law is chosen as

$$\boldsymbol{u} = -[K]\delta\boldsymbol{R} - [P]\delta\dot{\boldsymbol{R}} + \ddot{\boldsymbol{R}}_r - [f_R], \tag{38}$$

where [P] is a positive definite gain matrix. This control law results in the negative semi-definite Lyapunov rate

$$\dot{V}_1(\delta\boldsymbol{R}, \delta\dot{\boldsymbol{R}}) = -\delta\dot{\boldsymbol{R}}^T[P]\delta\dot{\boldsymbol{R}} \tag{39}$$

and closed loop tracking dynamics

$$\delta\ddot{\boldsymbol{R}} + [P]\delta\dot{\boldsymbol{R}} + [K]\delta\boldsymbol{R} = \boldsymbol{0}. \tag{40}$$

To examine asymptotic stability, higher-order derivatives are taken and evaluated on the set $\delta\dot{\boldsymbol{R}} = \boldsymbol{0}$.[17] The first non-zero derivative is found to be

$$\dddot{V}_1(\delta\boldsymbol{R}, \delta\dot{\boldsymbol{R}} = \boldsymbol{0}) = -2\delta\boldsymbol{R}^T[K]^T[P][K]\delta\boldsymbol{R} \tag{41}$$

which is negative definite in terms of $\delta\boldsymbol{R}$. Thus, the control law tracks the reference trajectory asymptotically. Furthermore, the asymptotic stability is global, due to the radially unbounded nature of the candidate Lyapunov function in Eq. (34).

The control law in Eq. (38) does not linearize the dynamics of L and $\hat{\boldsymbol{e}}$. Rather, it provides linear closed-loop tracking error dynamics. Using the unit-vector description, the preceding control law development provides a means to track an arbitrary, potentially time-varying reference trajectory. Its major drawback, however, is that it does not isolate the actuation of the separation distance from the relative orientation. For collision avoidance applications, it would be useful to be able to stabilize the relative separation distance more rapidly than relative orientation. This would allow for reorientation maneuvers which occur at a safely maintained separation distance. Indeed, one may argue that little is gained using this control law versus a similar development using Cartesian Hill frame coordinates. After all, this control law is essentially actuating on these Hill-frame coordinates directly, albeit with a different description. While perhaps not ideal, these developments illustrate that it is possible to track an arbitrary reference trajectory using the unit-vector description.

IV.A.2 Isolating L and $\hat{\boldsymbol{e}}$: γ Control Law

For the next control development, the problem of isolating the separation distance actuation capabilities from the relative orientation is considered. That is, a control law is sought which would allow for tracking of some reference L_r more quickly than a reference orientation $\hat{\boldsymbol{e}}_r$. Such a control would stabilize the relative separation distance early on in the maneuver before a large reorientation has occurred, thus minimizing the chance of collision. Rather than attempting to control all states of the system, only the separation distance and two elements of the unit-vector are considered. As an example, consider an orientation error measure defined by e_1 and e_2. If the control is tracking a reference e_{1r} and e_{2r}, then

$$e_1^2 + e_2^2 + e_3^2 = 1 = e_{1r}^2 + e_{2r}^2 + e_{3r}^2. \tag{42}$$

Because $e_1 = e_{1r}$ and $e_2 = e_{2r}$ once the system has converged to the reference, it is guaranteed that

$$e_3 \rightarrow \pm e_{3r}. \tag{43}$$

Thus, the system may converge to a state that is at the proper separation distance, but not at the proper orientation. A similar argument may be repeated for any of the other pairs of unit-vector components. Determination of the conditions required for convergence to the proper value is left for future work.

To arrive at a control law which isolates the separation distance from the relative orientation, consider the error measure $\delta\boldsymbol{\gamma}$, defined as

$$\delta\boldsymbol{\gamma} = \boldsymbol{\gamma} - \boldsymbol{\gamma}_r = \begin{bmatrix} L \\ e_i \\ e_j \end{bmatrix} - \begin{bmatrix} L_r \\ e_{ir} \\ e_{jr} \end{bmatrix}, \tag{44}$$

where e_i and e_j denote any two components of $\hat{\boldsymbol{e}}$. This error measure is used to define the candidate Lyapunov function

$$V_2(\delta\boldsymbol{\gamma}, \delta\dot{\boldsymbol{\gamma}}) = \frac{1}{2}\delta\boldsymbol{\gamma}^T[K]\boldsymbol{\gamma} + \frac{1}{2}\delta\dot{\boldsymbol{\gamma}}^T\delta\dot{\boldsymbol{\gamma}}, \tag{45}$$

where $[K]$ is a positive definite gain matrix. The derivative of this Lyapunov function is

$$\dot{V}_2(\delta\boldsymbol{\gamma}, \delta\dot{\boldsymbol{\gamma}}) = \delta\dot{\boldsymbol{\gamma}}^T\left([K]\delta\boldsymbol{\gamma} + \ddot{\boldsymbol{\gamma}} - \ddot{\boldsymbol{\gamma}}_r\right). \tag{46}$$

The differential equation for $\boldsymbol{\gamma}$ is

$$\ddot{\boldsymbol{\gamma}} = [f_\gamma] + [G_\gamma]\boldsymbol{u}, \tag{47}$$

where the elements of $[f_\gamma]$ and $[G_\gamma]$ are populated from Eq. 18 depending on which components of $\hat{\boldsymbol{e}}$ are used. Substituting these dynamics back into the Lyapunov rate expression yields

$$\dot{V}_2(\delta\boldsymbol{\gamma}, \delta\dot{\boldsymbol{\gamma}}) = \delta\dot{\boldsymbol{\gamma}}^T\left([K]\delta\boldsymbol{\gamma} + [f_\gamma] + [G_\gamma]\boldsymbol{u} - \ddot{\boldsymbol{\gamma}}\right). \tag{48}$$

To ensure stability, the control requirement used for the system is

$$[G_\gamma]\boldsymbol{u} = -[f_\gamma] - [K]\delta\boldsymbol{\gamma} - [P]\delta\dot{\boldsymbol{\gamma}} + \ddot{\boldsymbol{\gamma}}_r, \tag{49}$$

where $[P]$ is a positive definite gain matrix. This results in the negative semidefinite Lyapunov rate

$$\dot{V}_2(\delta\boldsymbol{\gamma}, \delta\dot{\boldsymbol{\gamma}}) = -\delta\dot{\boldsymbol{\gamma}}^T[P]\delta\dot{\boldsymbol{\gamma}}. \tag{50}$$

As before, asymptotic stability is determined through consideration of higher order derivatives of V_2.[17] Evaluated on the set $\delta\dot{\boldsymbol{\gamma}} = \boldsymbol{0}$, the first non-zero derivative is

$$\dddot{V}_2(\delta\boldsymbol{\gamma}, \delta\dot{\boldsymbol{\gamma}} = \boldsymbol{0}) = -2\delta\boldsymbol{\gamma}^T[K]^T[P][K]\delta\boldsymbol{\gamma}, \tag{51}$$

which is negative definite in terms of $\delta\boldsymbol{\gamma}$. Thus, if Eq. (49) is satisfied the system is asymptotically stable. The region of stability is global, due to the radially unbounded nature of V_2.

In order to find the control acceleration, $[G_\gamma]$ must be inverted and multiplied by the right hand side of Eq. (49). This presents a problem, however, as $[G_\gamma]$ is not always invertible. The nature of this singularity becomes evident when considering the determinant of $[G_\gamma]$. It is solely a function of L and e_k,

$$|[G_\gamma]| = \frac{e_k}{L^2}, \tag{52}$$

where e_k is the component of $\hat{\boldsymbol{e}}$ **not** used in $\boldsymbol{\gamma}$. If relative motion is desired in the chief orbit plane, for example, e_1 and e_2 cannot be used in $\boldsymbol{\gamma}$ or $[G_\gamma]$ will be singular all along the reference trajectory, where $e_3 = 0$.

The singularity issue is a very significant drawback to using this second control law to track a reference trajectory. If e_1 and e_2 are used in $\boldsymbol{\gamma}$, any trajectory that crosses from one side of the chief orbital plane to the other will encounter a singularity at the moment of crossing. If e_2 and e_3 are used in $\boldsymbol{\gamma}$, a trajectory that moves from above to below the chief (or vice-versa) will pass through the singularity. Lastly, if e_1 and e_3 are used in $\boldsymbol{\gamma}$, any trajectory that passes from in front to behind the chief (or vice-versa) will encounter the singularity issues. These conditions are extremely limiting on the number of reference trajectories that may be followed, and the performance of the system is very dependent on the starting location of the deputy. If the deputy is able to reach and converge onto the reference trajectory before a singularity is encountered then no problems will occur. However, for arbitrary reference motion and initial deputy conditions this is unlikely to be the case.

Let us turn our attention to a specific example of converging onto a naturally occurring relative motion. It is well known that for close separation distances, a naturally occurring relative motion is a 2x1 ellipse in the chief orbit plane. We will assume, at least for this example, that the ellipse is centered on the chief. It would not be possible to use e_1 and e_2 in $\boldsymbol{\gamma}$ for this case due to the fact that $e_3 = 0$ all along the reference trajectory. Thus, it would be required to use e_3 and either e_1 or e_2 in $\boldsymbol{\gamma}$. However, both e_1 and e_2 will pass through 0 twice during each revolution of the ellipse. This example illustrates how significant the singularity issues are, even in enforcing simple, naturally occurring motion.

The second major issue is the indeterminacy of e_k. There is no guarantee that the relative orientation will converge to the reference. It is likely that if the deputy starts closer to e_{kr} than $-e_{kr}$ that it will converge to the proper orientation, but there is no guarantee. Furthermore, note that to converge from a position near e_{kr} onto $-e_{kr}$, the system would have to pass through the singularity. For example, assume that e_3 is not used in $\boldsymbol{\gamma}$. If e_{3r} is a positive value, and $e_3(t_0)$ is also positive, the only way the system could converge to $-e_{3r}$ is if e_3 passed through the singularity at 0.

IV.B σ Set Control

The $\boldsymbol{\sigma}$ set is a minimal description. That is, three parameters are used to describe motion in a three-dimensional system. The problem of overdetermination that affected the unit-vector control law development is not an issue here. To develop a $\boldsymbol{\sigma}$-based control law the error parameter $\delta\boldsymbol{\zeta}$ is used, where

$$\delta\boldsymbol{\zeta} = \boldsymbol{\zeta} - \boldsymbol{\zeta}_r = \begin{bmatrix} L \\ \boldsymbol{\sigma} \end{bmatrix} - \begin{bmatrix} L_r \\ \boldsymbol{\sigma}_r \end{bmatrix}. \tag{53}$$

Consider the candidate Lyapunov function

$$V_3(\delta\boldsymbol{\zeta}, \delta\dot{\boldsymbol{\zeta}}) = \frac{1}{2}\delta\boldsymbol{\zeta}^T[K]\delta\boldsymbol{\zeta} + \frac{1}{2}\delta\dot{\boldsymbol{\zeta}}^T\delta\dot{\boldsymbol{\zeta}} \tag{54}$$

where $[K]$ is a positive definite gain matrix. The derivative of this Lyapunov function is

$$\dot{V}_3(\delta\boldsymbol{\zeta}, \delta\dot{\boldsymbol{\zeta}}) = \delta\dot{\boldsymbol{\zeta}}^T\left([K]\delta\boldsymbol{\zeta} + \ddot{\boldsymbol{\zeta}} - \ddot{\boldsymbol{\zeta}}_r\right).$$

Substituting in Eq. (26) yields

$$\dot{V}_3(\delta\boldsymbol{\zeta}, \delta\dot{\boldsymbol{\zeta}}) = \delta\dot{\boldsymbol{\zeta}}^T\left([K]\delta\boldsymbol{\zeta} + [h] + [G_\sigma]\boldsymbol{u} - \ddot{\boldsymbol{\zeta}}_r\right).$$

To ensure Lyapunov stability, the control law

$$\boldsymbol{u} = [G_\sigma]^{-1}\left(-[K]\delta\boldsymbol{\zeta} - [P]\delta\dot{\boldsymbol{\zeta}} - [h] + \ddot{\boldsymbol{\zeta}}_r\right)$$

is chosen, where $[P]$ is a positive definite gain matrix. This reduces the Lyapunov rate to

$$\dot{V}_3(\delta\boldsymbol{\zeta}, \delta\dot{\boldsymbol{\zeta}}) = -\delta\dot{\boldsymbol{\zeta}}^T[P]\delta\dot{\boldsymbol{\zeta}},$$

which is negative semi-definite. To determine asymptotic stability, higher order derivatives of the Lyapunov function are taken and evaluated on the set $\delta\dot{\boldsymbol{\zeta}} = 0$.[17] The first non-zero derivative is

$$\dddot{V}_3(\delta\boldsymbol{\zeta}, \delta\dot{\boldsymbol{\zeta}}) = -2\delta\boldsymbol{\zeta}^T[K]^T[P][K]\delta\boldsymbol{\zeta},$$

Table 1: Orbit elements for chief and deputy craft

	a (km)	e	i ($^\circ$)	Ω ($^\circ$)	ω ($^\circ$)	M_0 ($^\circ$)
Chief	7500	0	20	10	250	0
Deputy	a_c+0.05	$e_c + 0.00001$	$i_c - 0.001$	Ω_c	$\omega_c + 0.0001$	$M_{0,c}$

which is negative definite in terms of $\delta\boldsymbol{\zeta}$. Thus, the control law tracks the reference trajectory asymptotically.

The act of switching between original and shadow set has important implications for the control response. The preceding Lyapunov stability analysis assumes that V_3 and its derivatives are continuous. Switching to the shadow set violates this continuity assumption. Furthermore, the signs of L and L_r may present problems. If $L < 0$ and $L_r > 0$, for instance, the control law will strive to move the deputy through $L = 0$ to positive values where it will track L_r. Not only is this a collisional hazard, but passing through $L = 0$ is a singularity for the $\boldsymbol{\sigma}$ set.

Each of these issues may be addressed by switching the reference trajectory to its shadow set, so that the signs of L and L_r are always the same. If the deputy position description is switched from original to shadow set, then the reference trajectory must be switched as well. While the Lyapunov function is not continuous under this switching, it may be considered as a series of ever-decreasing functions. At each switching time, there is effectively a new function which will decrease with time until another switching occurs. As the original $\boldsymbol{\sigma}$ set moves closer to the reference, the shadow sets will also converge until tracking is achieved.

There is a potential issue with switching the reference trajectory to its shadow set. It is possible that the reference trajectory may be switched onto a singularity. Consider the following example. If the reference location is at $x = -50$ m in the Hill frame, the only defined $\boldsymbol{\sigma}$ set description for this position is $L = -50$ m, $\boldsymbol{\sigma} = \mathbf{0}$. If the deputy motion calls for the reference trajectory to switch to its shadow set, it will shift onto the singularity.

V Numerical Simulation

To validate and illustrate the performance of the unit-vector and $\boldsymbol{\sigma}$ set control laws, numerical simulation is used. Each of the control laws are implemented into an inertial simulation. For the inertial simulation, the trajectory of each craft is determined from integration of

$$\ddot{\boldsymbol{r}}_i = -\frac{\mu}{r^3}\boldsymbol{r}_i + \boldsymbol{u}, \tag{55}$$

where $\boldsymbol{u}$ is determined from the control laws developed above. The relative motion is then computed using the inertial trajectories of each craft. The initial conditions for each simulation are determined by defining a set of orbital elements for the chief, and orbit element differences for the deputy. Because the unit-vector and $\boldsymbol{\sigma}$ set equations of motion are obtained from the linearized CW equations, the orbital element differences will be kept at small levels such that the linear approximation is valid.

V.A Unit-vector γ Control Law

To demonstrate the performance of the unit-vector γ control law, a time-varying reference trajectory is prescribed in the Hill frame and the control law is applied to track the reference. The target reference motion, which is not a naturally occurring motion, is

$$x_r(t) = 0.05\cos(nt) \text{ (km)} \tag{56a}$$
$$y_r(t) = 0.05\sin(nt) \text{ (km)} \tag{56b}$$
$$z_r(t) = 0.02\sin(2nt + \pi/2) + 0.03 \text{ (km)}. \tag{56c}$$

The z coordinate is maintained positive to avoid singularity issues that would occur for the case when e_3 would pass from negative (-z) to positive ($+z$). The reference trajectory is transformed into unit-vector components for implementation into the control law, with gains of $[K] = n^2\text{diag}([10; 1; 1])$ and $[P] = n * \text{diag}([10; 1; 1])$. Gain selection is important for this scenario. Improper gain selection will cause the system to encounter the singular transition from +z to $-z$. Here, appropriate gains are chosen to avoid encountering the singularity and illustrate proper functionality of the control law.

The $\boldsymbol{\gamma}$ control law is applied using L, e_1, and e_2 for the error measure. By weighting the separation distance error 10 times higher than the relative orientation error, the singularity is avoided. The time histories of L and $\hat{e}$ during the maneuver are shown in Figure 5, and the state errors are presented in Figure 6. Due to the higher gains on the L error, the rate of converge to the reference separation distance is faster than the rate of convergence to the reference orientation.

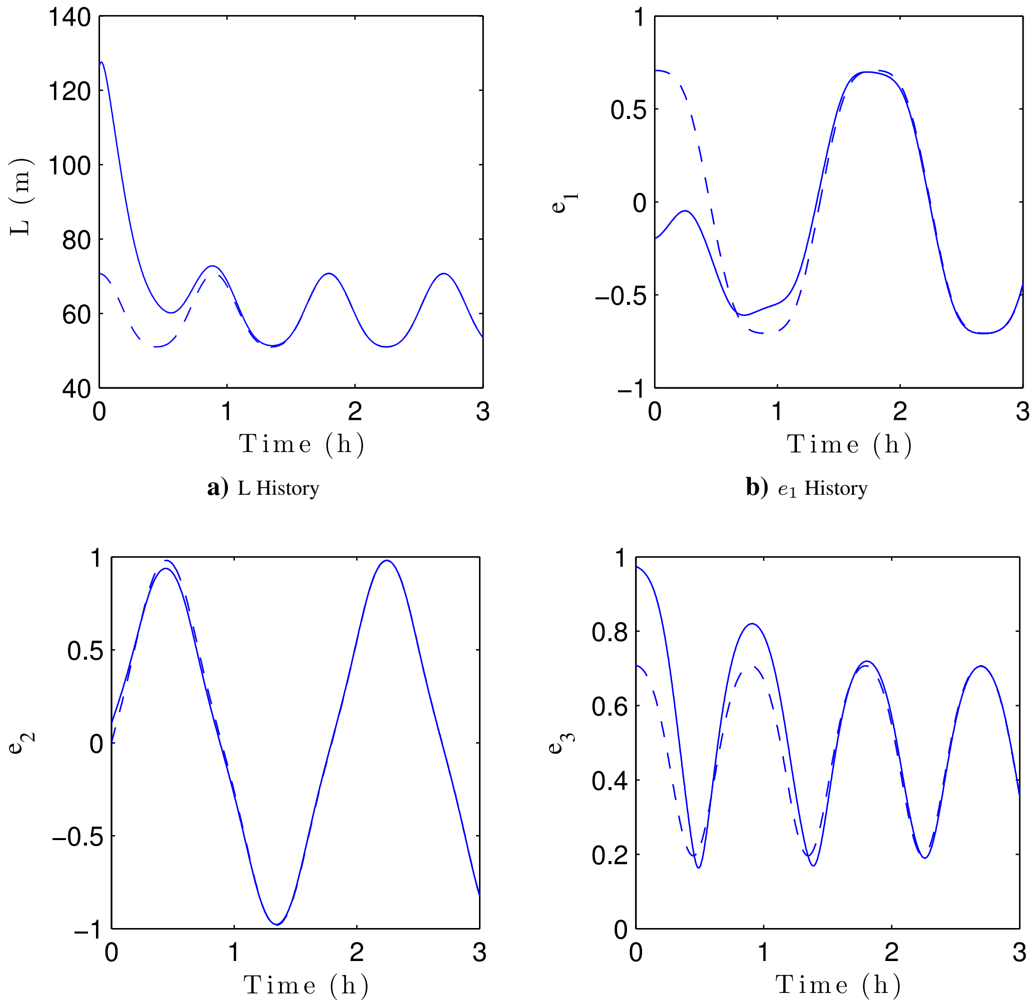

a) L History **b)** e_1 History **c)** e_2 History **d)** e_3 History

Figure 5: Time histories of L and $\hat{e}$ during tracking maneuver. The reference trajectory is shown as a dashed line.

The control inputs generated by the γ control law are shown in Figure 7. The transient response necessary for the deputy to reach the reference trajectory is evident, followed by the non-zero control required to maintain the non-naturally occurring reference motion. The magnitude of control acceleration needed is on the order of mm/s^2.

V.B σ Set Control Law

A major advantage of the $\boldsymbol{\sigma}$ set description is that it isolates the separation distance from the relative orientation. Using proper gain selection, a desired separation distance may be achieved quickly and maintained during reorientation. For example, if the deputy is to be repositioned from ahead to behind the chief, a safe separation distance may be maintained while the deputy moves around the chief. To illustrate this point, gains are chosen that cause the deputy to track the reference separation distance (L_r) more quickly than the relative orientation ($\boldsymbol{\sigma}$). The $\boldsymbol{\sigma}$ set control law developed above effectively linearizes the closed-loop dynamics into the form

$$\delta\ddot{\boldsymbol{\zeta}} + [P]\delta\dot{\boldsymbol{\zeta}} + [K]\boldsymbol{\zeta} = 0.$$

By choosing diagonal $[K]$ and $[P]$ gain matrices, the response of the system for L-tracking is independent of $\boldsymbol{\sigma}$-tracking. Here, a slightly underdamped response is desired with a damping ratio of $\zeta = 0.925$. For this system the

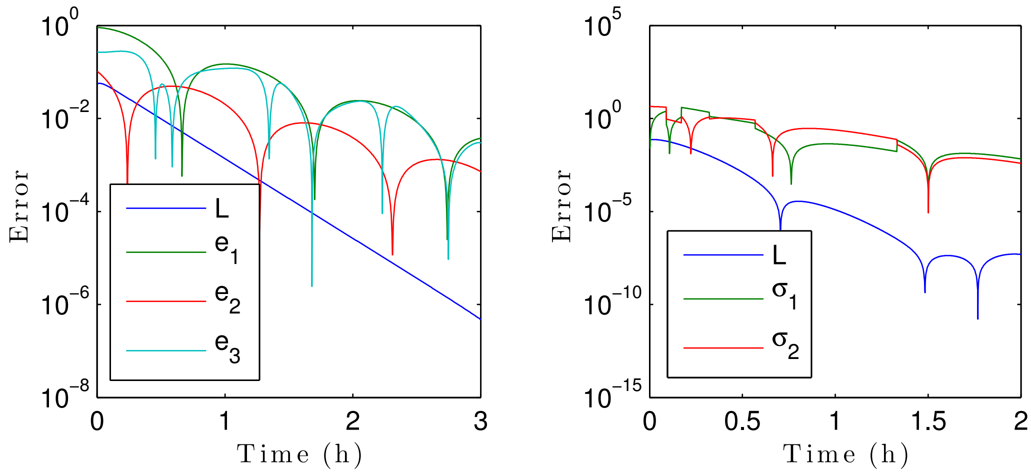

a) γ Control Law **b)** $\boldsymbol{\sigma}$ Set Control Law

Figure 6: State errors for unit-vector and $\boldsymbol{\sigma}$ set control laws throughout tracking maneuvers.

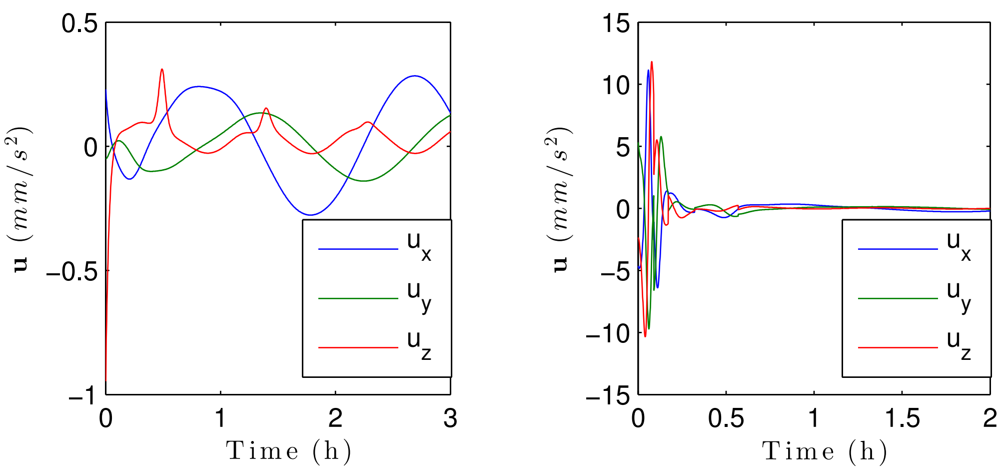

a) γ Control Law **b)** $\boldsymbol{\sigma}$ Set Control Law

Figure 7: Control inputs for unit-vector γ control law and $\boldsymbol{\sigma}$ set control law.

desired gains for a given settling time, T_s, are computed as[5, 18]

$$K_i = \frac{27.829}{T_s^2}$$
$$P_i = 1.85\sqrt{K_i}.$$

The settling time for L is chosen as 30 minutes, while the settling times for $\hat{e}$ and $\boldsymbol{\sigma}$ are chosen as 1 hour.

To illustrate tracking performance, once again a time varying trajectory is specified in Hill-frame coordinates. The trajectory used is

$$x_r(t) = 0.05\cos(nt)\ (\text{km}) \tag{57a}$$
$$y_r(t) = 0.05\sin(nt)\ (\text{km}) \tag{57b}$$
$$z_r(t) = 0.02\sin(2nt + \pi/2)(\text{km}). \tag{57c}$$

During the simulation the switching conditions of $|\boldsymbol{\sigma}| = 1$ is employed, and the reference trajectory is switched to its shadow set during every deputy switch so that sign(L) = sign(L_r). The time histories of L and $\boldsymbol{\sigma}$ during the maneuver are shown in Figure 8. The state errors over the same time period are shown in Figure 6. The switching times are

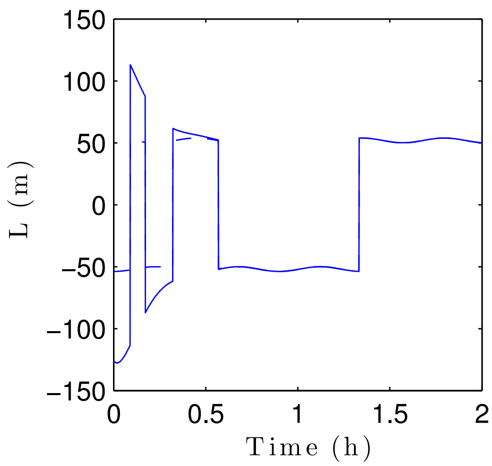

a) L History

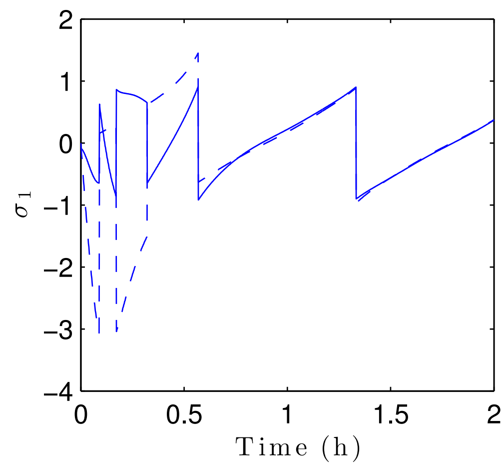

b) σ_1 History

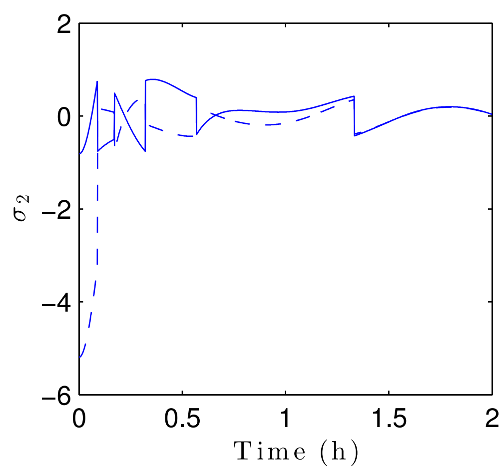

c) σ_2 History

Figure 8: Time histories of L and $\boldsymbol{\sigma}$ during tracking maneuver. The reference trajectory is shown as a dashed line.

evident, both for the actual and reference trajectories. While the magnitude of $\boldsymbol{\sigma}$ is constrained to be less than 1, the magnitude of $\boldsymbol{\sigma}_r$ is not. The reason is due to the fact that $\boldsymbol{\sigma}_r$ is automatically switched to its shadow set when $|\boldsymbol{\sigma}|$ calls for it, regardless of whether or not $|\boldsymbol{\sigma}_r| \leq 1$.

The effects of gain selection on the system response are clear in Figure 6. The separation distance has a rate of convergence to the reference that is twice as fast as the rate of convergence for $\boldsymbol{\sigma}$. The practical application for such a response is maintaining a safe separation distance during a reorientation maneuver. The control history for the $\boldsymbol{\sigma}$ set control law is shown in Fig 7. Again, mm/s^2 level control inputs are needed and a non-zero control is required to track the reference trajectory.

VI Conclusion

Two new relative motion descriptions are developed that are inspired by attitude parameter sets. The unit-vector description and $\boldsymbol{\sigma}$ set both isolate the separation distance from relative orientation. Equations of motion using these new descriptions are derived from the well-known Clohessy-Wiltshire equations. Reference trajectory tracking control laws are developed and implemented in numeric simulation. The unit-vector description is non-singular, and the $\boldsymbol{\sigma}$ set can avoid singularities by switching to its shadow set. However, the control laws developed for these descriptions may encounter unavoidable singularities. The issues present in the unit-vector γ control law are due to the fact that the description is overdetermined. That is, a four dimensional system is actuated upon by a three dimensional control vector. WIth the $\boldsymbol{\sigma}$ set, the control singularities are due to the fact that when a switch to the shadow set is called for, the reference trajectory must be switched as well. While the $\boldsymbol{\sigma}$ set is switched in such a way as to avoid singularities, the same cannot be said about the reference trajectory. Because the reference switching is dependent on the actual deputy trajectory, a switch may be called for that places the reference trajectory right on a singular orientation. Careful planning may be required to prevent issues from affecting control system performance.

References

[1]Clohessy, W. H. and Wiltshire, R. S., "Terminal Guidance System for Satellite Rendezvous," *Journal of the Aerospace Sciences*, Vol. 27, No. 9, 1960, pp. 653–658.

[2]de Bruijn, F. J., Gill, E., and How, J., "Comparative Analysis of Cartesian and Curvilinear Clohessy-Wiltshire Equations," *22nd International Symposium on Space Flight Dynamics*, São José dos Campos, Brazil, February 28-March 04 2011.

[3]Breger, L. and How, J., "GVE-Based Dynamics and Control for Formation Flying Spacecraft," *2nd International Symposium on Formation Flying Missions and Technologies*, Washington, DC, September 14-16 2004.

[4]Jiang, F., Li, J., and Baoyin, H., "Approximate analysis for relative motion of satellite formation flying in elliptical orbits," *Celestial Mechanics and Dynamical Astronomy*, Vol. 98, 2007, pp. 31–66.

[5]Hogan, E. and Schaub, H., "Relative Motion Control for Two-Spacecraft Electrostatic Orbit Corrections," *AAS/AIAA Spaceflight Mechanics Meeting*, Girdwood, Alaska, July 31 – August 4 2011, Paper AAS 11–466.

[6]Schaub, H. and Moorer, D. F., "Geosynchronous Large Debris Reorbiter: Challengs and Prospects," *AAS Kyle T. Alfriend Astrodynamics Symposium*, Monterey, CA, May 17–19 2010.

[7]Schaub, H. and Jasper, L. E. Z., "Circular Orbit Radius Control Using Electrostatic Actuation for 2-Craft Configurations," *AAS/AIAA Astrodynamics Specialist Conference*, Girdwood, Alaska, July 31 – August 4 2011, Paper AAS 11–498.

[8]Bombardelli, C. and Pelaez, J., "Ion Beam Shepherd for Contactless Space Debris Removal," *AIAA Journal of Guidance, Control, and Dynamics*, Vol. 34, No. 3, May–June 2011, pp. 916–920, doi:10.2514/1.51832.

[9]Kitamura, S., "Large Space Debris Reorbiter using Ion Beam Irradiation," *61st International Astronautical Congress*, Prague, Czech Republic, Sept. 27 – Oct. 1 2010.

[10]Bombardelli, C., Urrutxua, H., Merino, M., Ahedo, E., Pelaez, J., and Olympio, J., "Dynamics of Ion-Beam Propelled Space Debris," *International Symposium on Space Flight Dynamics*, Sao Jose dos Campos, Brasil, Feb. 28 – March 4, 2011 2011.

[11]Wiener, T. F., *Theoretical Analysis of Gimballess Inertial Reference Equipment Using Delta-Modulated Instruments*, Ph.D. dissertation, Department of Aeronautics and Astronautics, Massachusetts Institute of Technology, Cambridge, MA, March 1962.

[12]Marandi, S. R. and Modi, V. J., "A Preferred Coordinate System and the Associated Orientation Representation in Attitude Dynamics," *Acta Astronautica*, Vol. 15, No. 11, 1987, pp. 833–843.

[13]Tsiotras, P., "On the Choice of Coordinates for Control Problems on SO(3)," *30th Annual Conference on Information Sciences and Systems*, Princeton University, March 20–22 1996, pp. 1238–1243.

[14]Schaub, H. and Junkins, J. L., "Stereographic Orientation Parameters for Attitude Dynamics: A Generalization of the Rodrigues Parameters," *Journal of the Astronautical Sciences*, Vol. 44, No. 1, 1996, pp. 1–19.

[15]Schaub, H. and Junkins, J. L., *Analytical Mechanics of Space Systems*, AIAA Education Series, Reston, VA, 2nd ed., October 2009.

[16]Schaub, H., Vadali, S. R., and Alfriend, K. T., "Spacecraft Formation Flying Control Using Mean Orbit Elements," *Journal of the Astronautical Sciences*, Vol. 48, No. 1, 2000, pp. 69–87.

[17]Mukherjee, R. and Chen, D., "Asymptotic Stability Theorem for Autonomous Systems," *Journal of Guidance, Control, and Dynamics*, Vol. 16, 1993, pp. 961–963.

[18]Nise, N. S., *Control Systems Engineering*, Wiley, 5th ed., 2008.